Josephson current transport through T-shaped double quantum dots

2008 J. Phys.: Condens. Matter 20 505202

(http://iopscience.iop.org/0953-8984/20/50/505202)

J. Phys.: Condens. Matter **20** (2008) 505202 (5pp) doi:10.1088/0953-8984/20/50/505202

Josephson current transport through T-shaped double quantum dots

Shu-guang Cheng and Qing-feng Sun

Beijing National Laboratory for Condensed Matter Physics and Institute of Physics, Chinese Academy of Sciences, Beijing 100190, People's Republic of China

E-mail: sunqf@aphy.iphy.ac.cn

Received 6 October 2008
Published 7 November 2008
Online at stacks.iop.org/JPhysCM/20/505202

Abstract

The Josephson current through T-shaped double quantum dots (TDQD) has been investigated theoretically using the non-equilibrium Green's function method. Hybridization of energy levels of the central quantum dot (QD) and side QD results in the renormalization of Andreev bound states, which dominates the Josephson current. Consequently, Josephson critical current can be modulated to interference construction and destruction by adjusting the energy levels of two QDs ε_1, ε_2, and interdot coupling t_c. In detail, when $\varepsilon_1\varepsilon_2 = t_c^2$ is fulfilled, interference construction occurs and when $\varepsilon_2 = 0$, interference destruction happens. These results are similar to the interference behavior of linear conductance in normal TDQD devices. In addition, Josephson critical current also shows Fano characteristics with variation of ε_2 and the resonance line shape is determined by ε_1. Finally, the Josephson current has a symmetric relation of $I(\varepsilon_1, \varepsilon_2) = I(-\varepsilon_1, -\varepsilon_2)$ due to electron–hole symmetry.

1. Introduction

Owing to advances in nanotechnology, the interference of the transport of phase coherent electrons in mesoscopic devices has been widely researched in recent years [1–3]. It provides detectable quantum states within devices which facilitate novel fabrication of quantum apparatus. The Aharonov–Bohm (AB) interferometer, a typical interferometer, is more controllable if a quantum dot (QD) is embedded in one arm or each arm. An AB interferometer with two QDs inserted in two arms is useful for detecting electron interference and possible realization of two-electron spin entanglement [4]. In the situation of just one QD in one arm of an AB interferometer, the Fano effect, first proposed in atomic physics [5], can be observed and modulated by changing magnetic flux Φ through the ring or the energy level of the QD ε_d. The Fano effect arises from the interference between a continuum energy spectrum and discrete energy states. It shows a typical Fano resonance of transmission probability $T(E)$ as a function of the discrete energy level ε_d [6, 7]. Transmission probability is generally of the type $T(E) \propto \frac{(\epsilon+q)^2}{\epsilon^2+1}$, in which $\epsilon = \frac{E-\varepsilon_d}{\Gamma}$ and Γ is the coupling strength between QD and the leads. The Fano parameter q is generally a complex number which counts the characteristics of the corresponding model, and it determines the line shape of the resonance. What is more, the Fano effect in mesoscopic devices has been realized in experiments [8, 9] and has evoked other related topics such as the Kondo–Fano effect [10].

Similar to the Fano model of a QD in an AB interferometer, a QD with another QD side couple to it (as shown in figure 1), called the T-shaped double QD (TDQD) model, is another prototype of the Fano model. In this model, compared with the side QD which is not connected directly to the leads, the spectrum of electrons in the central QD connected to a source and a drain act as the continuum energy spectrum. Interference occurs by electron transport through two paths, one is tunneling through the central QD and the other is through the central QD and then with extra scattering by the side QD. The energy level of the side QD plays the role of a Fano resonance shape modulator, because an extra phase Θ_{QD} emerges when the electron is elastically scattered by the side QD [11]. Θ_{QD} is zero when the energy level of the side QD $\varepsilon_2 = 0$ and is $\pi/2$ $(-\pi/2)$ when $\varepsilon_2 \gg 0$ $(\varepsilon_2 \ll 0)$. So transport enhancement and suppression can be realized by adjusting the QDs' levels. Electron transport through the normal(N)-TDQD-N model has been widely researched. Güçlü and coworkers studied the TDQD when the side QD is a Kondo impurity and found suppression of the conductance [12]. Wu *et al* focused on the TDQD consisting of a central Kondo dot and a side coupled

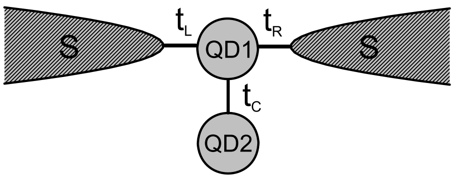

Figure 1. Schematic diagram for the TDQD system. QD1 is connected to two superconductor leads with coupling parameter t_L and t_R. QD2 is side coupled to QD1 with coupling parameter t_c.

noninteracting QD, and they found that linear conductance of Kondo unitary is broken down by the side QD [13, 14]. Cornaglia and Grempel showed that when both QDs are in the Kondo regime, conductance is controlled by interdot coupling and the Kondo temperature of QDs [15]. Tanamoto and Nishi researched the modulation of the Fano dip in a similar model with a side coupled QD molecular model [16]. Previous works all concentrate on the TDQD device coupled to normal contacts, while Josephson current through TDQD has not been investigated yet. When a TDQD is embedded between two superconductor (S) leads, the Cooper pairs could tunnel through the TDQD device even in the zero bias case because of the superconductor phase difference of the two leads. Interference of the Cooper pairs passing through the two paths should also happen. The interference construction and destruction, Fano effect of the Cooper pair transport, as well the characteristics of the Andreev bound states are the motivations behind this work.

In this paper we consider a TDQD structure connected to two superconductor leads. By using the non-equilibrium Green's function method, the Josephson current expression and Andreev bound states are obtained. The Andreev bound states are strongly affected by the side QD due to hybridization of two QD levels ε_1 and ε_2. While in weak coupling to the superconductor leads, the positions of the Andreev bound states are close to the molecular levels of isolated DQDs. The critical Josephson current I_c can be modulated to interference construction and destruction due to the interference of Cooper pair transport through two paths. In detail, when $\varepsilon_2 = 0$, I_c is suppressed and when relation $t_c^2 = \varepsilon_1\varepsilon_2$ is fulfilled, interference construction of Josephson current occurs. Fano type resonance of I_c is observed by adjusting ε_2 with the line shape depending on ε_1. When $\varepsilon_1 \neq 0$, typical asymmetric Fano resonance of I_c–ε_2 is found, whereas when $\varepsilon_1 = 0$, I_c–ε_2 is symmetric. Finally we found that the Josephson current has the property, $I(\varepsilon_1, \varepsilon_2) = I(-\varepsilon_1, -\varepsilon_2)$, which includes the electron–hole symmetry.

The rest of the paper is organized as follows. In section 2, the Hamiltonian and Josephson current expressions are presented. In section 3, we show our main numerical results of the Josephson current–superconducting phase relation, the Andreev bound states phase relation, the interference construction and destruction of critical current related to QD levels, and the Fano characteristics of the critical current. Finally a brief conclusion is given in section 4.

2. Model and formulations

We consider a TDQD structure connected to two Bardeen–Cooper–Schrieffer (BCS) superconductor leads as shown in figure 1. QD1 is connected to both superconductor leads with coupling parameters t_L and t_R respectively. QD2 is side coupled to QD1 with interdot coupling parameter t_c. The Hamiltonian of the system can be written as

$$H = \sum_{\alpha=L,R} H_\alpha + \sum_{i=1,2} H_i + H_t, \tag{1}$$

where H_α and H_i are the Hamiltonian of the αth superconductor lead and the ith QD, respectively. H_t is the tunneling term, including the coupling of QD1 to two superconductor leads and coupling between QD1 and QD2. Terms in equation (1) are expressed as:

$$\begin{aligned} H_\alpha &= \sum_{k\sigma} \varepsilon_k C^\dagger_{k\sigma,\alpha} C_{k\sigma,\alpha} \\ &\quad + \sum_k \Delta (C_{k\downarrow,\alpha} C_{-k\uparrow,\alpha} + C^\dagger_{-k\uparrow,\alpha} C^\dagger_{k\downarrow,\alpha}) \\ H_i &= \sum_\sigma \varepsilon_i d^\dagger_{i\sigma} d_{i\sigma} \\ H_t &= \sum_{k,\sigma,\alpha} (t_\alpha \mathrm{e}^{\frac{\mathrm{i}\theta_\alpha}{2}} C^\dagger_{k\sigma,\alpha} d_{1\sigma} + t_\alpha \mathrm{e}^{-\frac{\mathrm{i}\theta_\alpha}{2}} d^\dagger_{1\sigma} C_{k\sigma,\alpha}) \\ &\quad + t_c (d^\dagger_{1\sigma} d_{2\sigma} + d^\dagger_{2\sigma} d_{1\sigma}), \end{aligned} \tag{2}$$

where Δ and θ_α are the superconductor energy gap and phase. Here we have taken a unitary transformation as [17], so the superconductor phase θ_α emerges in the tunneling Hamiltonian H_t in equation (2). We consider single level QDs, and ε_i is the energy level of the ith QD. Here the electron–electron interaction in the QDs is neglected, because we consider the large QD. In fact, if the temperature is higher than the Kondo temperature, the electron–electron interaction is only to widen the space of the levels, and the results are qualitatively the same.

The current through the αth lead is calculated from the evolution of the electron number operator $N_\alpha = \sum_{k\sigma} C^\dagger_{k\sigma\alpha} C_{k\sigma\alpha}$ [18, 19],

$$\begin{aligned} I_\alpha = &\ -e\langle \dot{N} \rangle \\ = &\ \frac{4e}{\hbar} \mathrm{Re} \int \frac{\mathrm{d}E}{2\pi} t_\alpha \mathrm{e}^{\frac{\mathrm{i}\theta_\alpha}{2}} G^<_{1\alpha,11}(E) \end{aligned} \tag{3}$$

$\mathbf{G}^<_{1\alpha}(E)$ is the Fourier transformation of $\mathbf{G}^<_{1\alpha}(t - t')$, and

$$\mathbf{G}^<_{1\alpha}(t-t') \equiv \mathrm{i} \sum_k \begin{pmatrix} \langle C^\dagger_{k\uparrow,\alpha}(t') d_{1\uparrow}(t) \rangle & \langle C_{-k\downarrow,\alpha}(t') d_{1\uparrow}(t) \rangle \\ \langle C^\dagger_{k\uparrow,\alpha}(t') d^\dagger_{1\downarrow}(t) \rangle & \langle C_{-k\downarrow,\alpha}(t') d^\dagger_{1\downarrow}(t) \rangle \end{pmatrix}$$

under the Nambu representation.

We consider here the dc Josephson effect, thus $\mathbf{G}^<_{1\alpha}(E)$ can be simplified by the fluctuation-dissipation theorem that $\mathbf{G}^<_{1\alpha} = -f(E)(\mathbf{G}^r_{1\alpha}(E) - \mathbf{G}^a_{1\alpha}(E))$ and $f(E)$ is the Fermi–Dirac distribution and $\mathbf{G}^{r,a}_{1\alpha}(E)$ are the retarded and advanced Green's functions.

By using Dyson's equation, the retarded Green's function $\mathbf{G}^r_{1\alpha}(E)$ can be expressed as $\mathbf{G}^r_{1\alpha} = \mathbf{G}^r_1 \mathbf{t}^*_\alpha \mathbf{g}^r_\alpha$, and the Green's function $\mathbf{G}^r_1$ of QD1 is $\mathbf{G}^r_1 = (\mathbf{g}^{-1}_1 - \mathbf{\Sigma}^r)^{-1}$. $\mathbf{\Sigma}^r = \mathbf{t}^*_L \mathbf{g}^r_L \mathbf{t}_L + \mathbf{t}^*_R g^r_R \mathbf{t}_R + \mathbf{t}^*_c \mathbf{g}^r_2 \mathbf{t}_c$ is the retarded self-energy

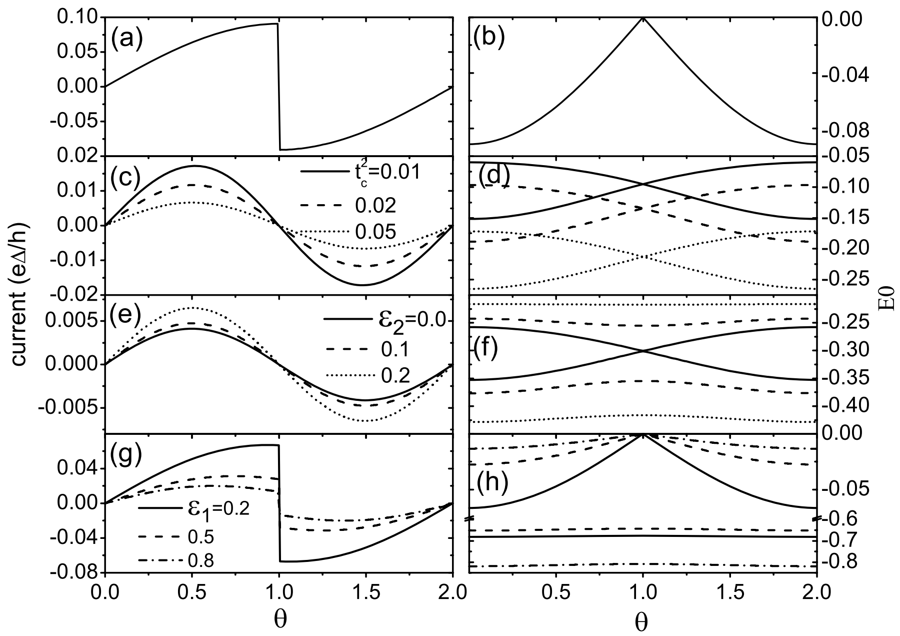

Figure 2. Left panel: Josephson current I versus superconductor phase θ for various parameters, (a) $t_c = 0$, $\Gamma = 0.1$ and $\varepsilon_1 = 0$; (c) $\varepsilon_1 = \varepsilon_2 = 0$ and $\Gamma = 0.1$ for different QD coupling t_c; (e) $\varepsilon_1 = 0$, $\Gamma = t_c^2 = 0.1$ for different ε_2 values; (g) $\Gamma = t_c^2 = 0.1$ and ε_1, ε_2 satisfies $\varepsilon_1\varepsilon_2 = t_c^2$. Right panel: Andreev bound states versus superconductor phase θ with the parameters corresponding to the left panel.

coupled to superconductor leads and QD2. Here $\mathbf{g}_\alpha^r(E)/\mathbf{g}_i^r(E)$ is the Green's function of the isolated superconductor lead or the Green's function of the isolated ith QD, and $\mathbf{t}_\alpha/\mathbf{t}_c$ is the tunneling matrix corresponding to t_α/t_c in the Nambu representation. The expression of $\mathbf{g}_\alpha^r(E)$ is [20] $\mathbf{g}_\alpha^r(E) = -\pi\rho(E)\begin{pmatrix}\beta(E) & \beta_0(E)\\ \beta_0(E) & \beta(E)\end{pmatrix}$ and $\mathbf{g}_i^r(E) = \begin{pmatrix}1/(E-\varepsilon_i+\mathrm{i}\eta) & 0\\ 0 & 1/(E+\varepsilon_i+\mathrm{i}\eta)\end{pmatrix}$, where $\rho(E)$ is the normal density of states of the superconductor lead, $\beta_0(E) = \beta\Delta/E$, and $\beta(E) = E/\sqrt{\Delta^2-E^2}$ while $|E| < \Delta$ and $\beta(E) = \mathrm{i}|E|/\sqrt{E^2-\Delta^2}$ while $|E| > \Delta$. Tunneling matrices are $\mathbf{t}_\alpha = t_\alpha\begin{pmatrix}\mathrm{e}^{\mathrm{i}\theta_\alpha/2} & 0\\ 0 & -\mathrm{e}^{-\mathrm{i}\theta_\alpha/2}\end{pmatrix}$ and $\mathbf{t}_c = t_c\begin{pmatrix}1 & 0\\ 0 & -1\end{pmatrix}$. For convenience we take the symmetric barriers with $t_L = t_R$ and $\theta_L = -\theta_R = \theta/2$.

Finally we have the reduced Josephson current expression

$$I_\alpha = \frac{-2e}{\hbar}\int \frac{\mathrm{d}E}{2\pi} f(E)\frac{\beta_0^2\Gamma^2\sin\theta}{\mathrm{Im}\{B\}}, \qquad (4)$$

where $B = (E - \frac{Et_c^2}{E^2-\varepsilon_1^2} + \Gamma\beta)^2 - (\varepsilon_1 + \frac{\varepsilon_2 t_c^2}{E^2-\varepsilon_2^2})^2 - \Gamma^2\beta_0^2\cos^2\frac{\theta}{2}$, and the linewidth function $\Gamma \equiv 2\pi\rho t_\alpha^2$ describes the coupling strength of QD1 to the superconductor leads, which is assumed independent of the energy E.

Two parts contribute to the Josephson current, the continuous part I_{con} arises from electrons of energy E outside the superconducting gap Δ and the discrete part I_{dis} from electrons of energy within the gap Δ. The continuous part I_{con} is obtained directly by the integral in equation (4), while the discrete part is approached by solving poles of factor B which are the Andreev bound states. Affected by the QD2, instead of one pair of bound states $\pm E_0$ in a S–QD–S junction, there are two pairs of Andreev bound states $E_{i=1,2}^{\pm}$ with $E_i^+ = -E_i^-$ and they all make contributions to the current. Besides, as in the S–QD–S Josephson junction, the current I_{dis} contributed by the Andreev bound states is usually much larger than the continuous part.

3. Results and discussion

In this section, we will present the numerical results on Josephson current–superconducting phase relations and the corresponding Andreev bound states–phase relations, the interference construction and destruction of critical current, as well as the Fano characteristics of critical current.

In figure 2 we show the current phase relation (I–θ) for different parameters and the corresponding Andreev bound states' phase relation ($E_i^{\pm}$–θ). These two relations are connected by $I_{\mathrm{dis}} = -\frac{2e}{\hbar}\sum_{i,\pm} f(E_i^{\pm})\frac{\partial E_i^{\pm}}{\partial\theta}$ [21, 22]. Because the bound states within the gap are paired with energy of opposite signs, we only show those in half-interval $[-\Delta, 0]$. First, by decoupling QD2, the usual S–QD–S junction is displayed in figure 2(a). When $\varepsilon_1 = 0$, the current shows a discontinuous jump at $\theta = \pi$ and meanwhile the Andreev bound states $\pm E_0$ degenerate at $E = 0$ [23–25]. When QD2 coupling is considered, I–θ is usually a sinuous line shape and the current is suppressed as t_c is increased (see figure 2(c)). In this case, the Andreev bound states depart from the Fermi energy $E_F = 0$ which breaks down the resonance and suppresses the current (see figure 2(d)). In figure 2(e), current for different ε_2 values is shown. The current is enhanced as ε_2 is away from the Fermi energy which illustrates that in $\varepsilon_2 = 0$ current is suppressed. Andreev bound states cross when $\varepsilon_2 = 0$ at $\theta = \pi$ and they depart from each other as ε_2 is away from the Fermi level. Finally in figure 2(g), the current jump at $\theta = \pi$ appears when the relation $\varepsilon_1\varepsilon_2 = t_c^2$ is fulfilled. Corresponding Andreev bound states in this condition display the same behavior as in figure 1(b) where one pair of

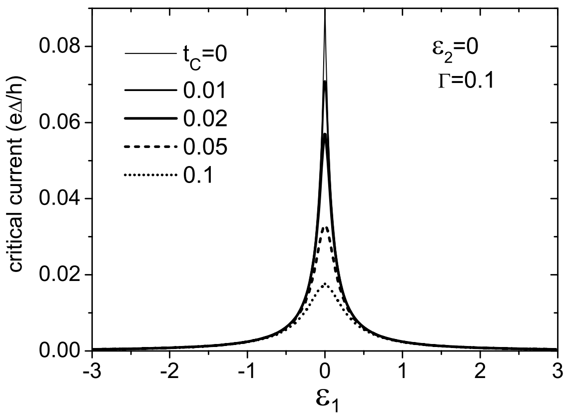

Figure 3. Critical current versus ε_1 for different interdot coupling t_c.

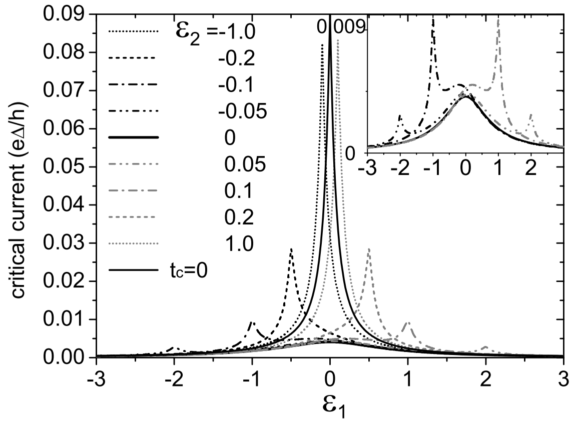

Figure 4. Critical current versus ε_1 for different ε_2 values with $t_c^2 = \Gamma = 0.1$. The curve for $t_c = 0$ is also shown for comparison. Inset: enlarged figure of critical current for the curves with $\varepsilon_2 = 0, \pm 0.05$ and ± 0.1.

bound states degenerates at $E = 0$ and the current carried by the bound states changes its sign abruptly [26]. This condition can be analytically obtained from the expression B. Supposing Andreev bound states degenerate at $E = 0$, by solving $B(E = 0) = 0$, we easily have

$$\varepsilon_1 \varepsilon_2 = t_c^2, \qquad \theta = \pi. \tag{5}$$

This means, if these two conditions hold, that the degeneration of one pair of bound states at the Fermi level will occur and consequently, a Josephson current jump at $\theta = \pi$ will occur as well. Besides, equation (5) is the condition for maximum critical current, which will be detailed in the following discussions.

Finally in this I–θ discussion, we note that in a N–TDQD–N, the realization of a linear conductance maximum is exactly equation (5). In fact, the values of Andreev bound states in our model when weakly coupled to S leads are very close to the molecular levels of the isolated QD molecule $\varepsilon^{\pm} = [(\varepsilon_1 + \varepsilon_2) \pm \sqrt{(\varepsilon_1 - \varepsilon_2)^2 + 4t_c^2}]/2$ (not shown here) which is also the resonance center of linear conductance in the N–TDQD–N model [13].

Next, we focus on the critical current through the TDQD. The critical current I_c is obtained by choosing the maximum Josephson current in a 2π period of superconductor phase θ. In figure 3 we plot I_c as an energy level of QD1 ε_1 for different interdot coupling t_c at $\varepsilon_2 = 0$. I_c shows a symmetric peak at $\varepsilon_1 = 0$, and this peak is strongly suppressed when t_c is introduced with even tiny values. This result can be understood from the interference of two paths. When ε_1 aligns the Fermi level, electrons are easy to transport through the system. However when QD2 is connected with its level $\varepsilon_2 = E_F = 0$, electrons being transported through QD1 tend to tunneling into QD2. Then interference destruction between two paths occurs, and the current is decreased. So, while level ε_2 closes to the Fermi level, QD2 acts as an impurity to scatter the incident electron or Cooper pair. This result resembles the transport through an N–TDQD–N device.

In figure 4, we plot the I_c–ε_1 relation for different ε_2. Here we also show a graph of $t_c = 0$ for comparison. For given t_c, I_c shows a peak at $\varepsilon_1 = 0$ when $\varepsilon_2 = 0$ (see the inset of figure 4). As ε_2 is moving off the Fermi level, interference construction begins to function. Consequently an extra peak

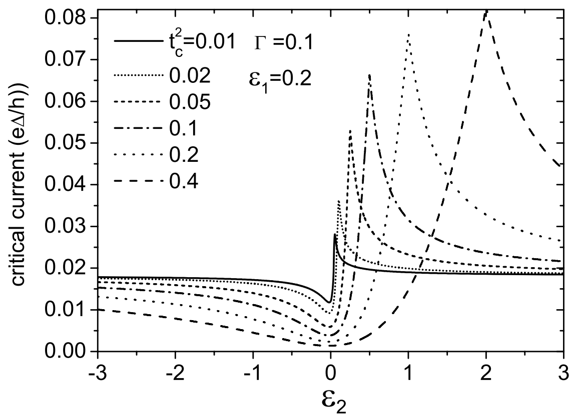

Figure 5. Critical current versus ε_2 for different interdot coupling t_c for nonzero ε_1. Other parameters are $\varepsilon_1 = 0.2$ and $\Gamma = 0.1$.

is shown and the original peak at $\varepsilon_1 = 0$ becomes obscure. The position of the extra peak is determined by equation (5). When equation (5) is satisfied, one pair of Andreev bound states aligns to the Fermi level which facilitates the transport. With ε_2 moving further off the Fermi level, or in other words, when QD2 is gradually isolated from QD1, the curve of I_c–ε_1 tends to that of the S–QD–S junction (i.e. the $t_c = 0$ case).

Now we focus on the Fano resonance characteristics of critical current. In figure 5 we plot a graph of I_c–ε_2 for different interdot coupling. I_c–ε_2 shows a typical Fano asymmetric line shape when $\varepsilon_1 \neq 0$. There is an obvious Fano valley at $\varepsilon_2 = 0$ and a peak depending on equation (5). With enhanced t_c, the interference destruction and construction are enhanced even more. The Fano valley is still at $\varepsilon_2 = 0$ with smaller critical current, but the peak is moved away with larger magnitude of the critical current.

Finally, we also found that the Fano line shape of critical Josephson current can be modulated by the QD1 level, which is like the Fano effect in an AB interferometer with its Fano line shape modulated by magnetic flux. In figure 6 we plot I_c–ε_2 for different ε_1 values. The curves show a valley at $\varepsilon_2 = 0$ and a peak at $\varepsilon_2 = t_c^2/\varepsilon_1$. In particular, with the change of ε_1,

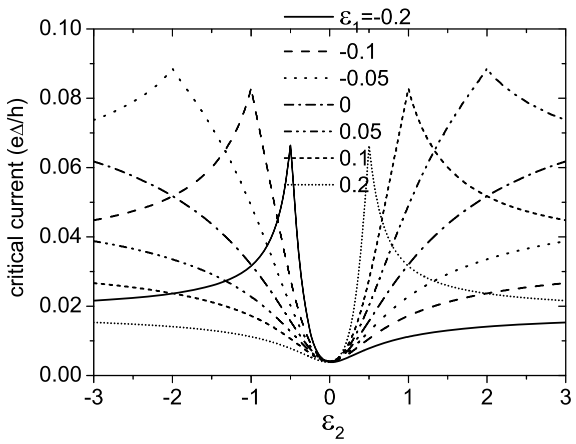

Figure 6. Critical current versus ε_2 for different ε_1. Other parameters are $t_c^2 = 0.1$ and $\Gamma = 0.1$.

the Fano peak can be modulated and the peak position can vary from the right side with $\varepsilon_2 > 0$ to the left side with $\varepsilon_2 < 0$. In addition, a relation $I_c(\varepsilon_1, \varepsilon_2) = I_c(-\varepsilon_1, -\varepsilon_2)$ is found from figure 6, which reflects the basic physics of electron–hole symmetry. In fact, by taking the transform d_i to $\tilde{d}_i^\dagger$ and simultaneously setting the parameters $(\varepsilon_1, \varepsilon_2)$ to $(-\varepsilon_1, -\varepsilon_2)$, the Hamiltonian H in formula (1) is invariable. So the Josephson current has the relation $I(\varepsilon_1, \varepsilon_2) = I(-\varepsilon_1, -\varepsilon_2)$.

4. Summary

The Josephson current through a T-shaped double quantum dot device has been investigated. Josephson critical current can be modulated by energy levels of two QDs ε_1 and ε_2. The interference construction occurs when interdot coupling t_c and energy levels fulfil $\varepsilon_1\varepsilon_2 = t_c^2$, and the interference destruction emerges while $\varepsilon_2 = 0$. Critical current versus the side QD level ε_2 shows Fano characteristics with resonance shape determined by the central QD ε_1. In addition, due to electron–hole symmetry, the Josephson current has the relation $I(\varepsilon_1, \varepsilon_2) = I(-\varepsilon_1, -\varepsilon_2)$.

Acknowledgments

We thank Professor Xie for many helpful discussions. We gratefully acknowledge the financial support from NSF-China under grant Nos 10525418 and 10734110.

References

[1] Bachtold A, Strunk C, Salvetat J P, Bonard J M, Forró L, Nussbaumer T and Schönenberger C 1999 *Nature* **397** 673
Ji Y, Heiblum M, Sprinzak D, Mahalu D and Shtrikman H 2000 *Science* **779** 290
[2] Ji Y, Heiblum M and Shtrikman H 2002 *Phys. Rev. Lett.* **88** 076601
[3] van der Wiel W G, De Franceschi S, Fujisawa T, Elzerman J M, Tarucha S and Kouwenhoven L P 2000 *Science* **289** 2105
[4] Hatano T, Stopa M and Tarucha S 2005 *Science* **309** 268
[5] Fano U 1961 *Phys. Rev.* **124** 1866
[6] Fuhrer A, Brusheim P, Ihn T, Sigrist M, Ensslin K, Wegscheider W and Bichler M 2006 *Phys. Rev.* B **73** 205326
Ueda A and Eto M 2006 *Phys. Rev.* B **73** 235353
[7] Sun Q-F, Wang J and Guo H 2005 *Phys. Rev.* B **71** 165310
[8] Kobayashi K, Aikawa H, Katsumoto S and Iye Y 2002 *Phys. Rev. Lett.* **88** 256806
Kobayashi K, Aikawa H, Katsumoto S and Iye Y 2003 *Phys. Rev.* B **68** 235304
Kobayashi K, Aikawa H, Sano A, Katsumoto S and Iye Y 2004 *Phys. Rev.* B **70** 035319
[9] Johnson A C, Marcus C M, Hanson M P and Gossard A C 2004 *Phys. Rev. Lett.* **93** 106803
[10] Bułka B R and Stefański P 2001 *Phys. Rev. Lett.* **86** 15128
Hofstetter W, König J and Schoeller H 2001 *Phys. Rev. Lett.* **87** 156803
[11] Schuster R, Buks E, Heiblum M, Mahalu D, Umansky V and Shtrikman H 1997 *Nature* **385** 420
Yacoby A, Heiblum M, Mahalu D and Shtrikman H 1995 *Phys. Rev. Lett.* **74** 4047
[12] Güçlü A D, Sun Q-F and Guo H 2003 *Phys. Rev.* B **68** 245323
[13] Wu B H, Cao J C and Ahn K-H 2005 *Phys. Rev.* B **72** 165313
[14] Liu Y S, Yang X F, Fan X H and Xia Y J 2008 *J. Phys.: Condens. Matter* **20** 135226
[15] Cornaglia P S and Grempel D R 2005 *Phys. Rev.* B **71** 075305
[16] Tanamoto T and Nishi Y 2007 *Phys. Rev.* B **76** 155319
[17] Sun Q-F, Wang B-G, Wang J and Lin T-H 2000 *Phys. Rev.* B **61** 4754
[18] Wingreen N S, Jauho A P and Meir Y 1993 *Phys. Rev.* B **48** 8487
[19] Wingreen N S, Jacobsen K W and Wilkins J W 1999 *Phys. Rev.* B **40** 11834
[20] Sun Q F, Wang J and Lin T H 1999 *Phys. Rev.* B **59** 3831
Sun Q F, Wang J and Lin T H 1999 *Phys. Rev.* B **59** 13126
[21] Beenakker C W J 1991 *Phys. Rev. Lett.* **67** 3836
[22] Bardeen J, Kümmel R, Jacobs A E and Tewordt L 1969 *Phys. Rev.* B **187** 556
[23] Ishii C 1970 *Prog. Theor. Phys.* **44** 1525
Bardeen J and Johnson J L 1972 *Phys. Rev.* B **5** 72
[24] Golubov A A, Kupriyanov M Yu and Il'ichev E 2004 *Rev. Mod. Phys.* **76** 411
[25] Devyatov I A and Kupriyanov M Yu 1997 *Zh. Eksp. Teor. Fiz.* **112** 342
Devyatov I A and Kupriyanov M Yu 1997 *JETP* **85** 189 (Engl. Transl.)
[26] Hurd M and Wendin G 1994 *Phys. Rev.* B **49** 15258